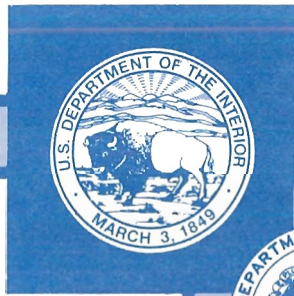**REPORT OF INVESTIGATIONS/1995**

In Situ Stress at the Lucky Friday Mine

(In Four Parts):

1. Reanalysis of Overcore Measurements From 4250 Level

By J. K. Whyatt and M. J. Beus

UNITED STATES DEPARTMENT OF THE INTERIOR

BUREAU OF MINES

U.S. Department of the Interior
Mission Statement

As the Nation's principal conservation agency, the Department of the Interior has responsibility for most of our nationally-owned public lands and natural resources. This includes fostering sound use of our land and water resources; protecting our fish, wildlife, and biological diversity; preserving the environmental and cultural values of our national parks and historical places; and providing for the enjoyment of life through outdoor recreation. The Department assesses our energy and mineral resources and works to ensure that their development is in the best interests of all our people by encouraging stewardship and citizen participation in their care. The Department also has a major responsibility for American Indian reservation communities and for people who live in island territories under U.S. administration.

In Situ Stress at the Lucky Friday Mine

(In Four Parts):

1. Reanalysis of Overcore Measurements From 4250 Level

By J. K. Whyatt and M. J. Beus

UNITED STATES DEPARTMENT OF THE INTERIOR
Bruce Babbitt, Secretary

BUREAU OF MINES
Rhea L. Graham, Director

CONTENTS

TABLES—Continued

UNIT OF MEASURE ABBREVIATIONS USED IN THIS REPORT

Metric Units

cm	centimeter	MPa	megapascal
GPa	gigapascal	pct	percent
m	meter	$\mu\epsilon$	microstrain
m/m	meter per meter		

U.S. Customary Units

ft	foot	psi	pound per square inch
in	inch		

IN SITU STRESS AT THE LUCKY FRIDAY MINE

(In Four Parts):

1. Reanalysis of Overcore Measurements From 4250 Level

By J. K. Whyatt[1] and M. J. Beus[1]

ABSTRACT

During the past 2 years, U.S. Bureau of Mines (USBM) researchers reviewed an in situ stress investigation conducted in 1977 at a test site on the 4250 level of the Lucky Friday Mine, Mullan, ID. Although the field measurements of overcore strain were found to be useful, significant deficiencies were found in the stress field estimation procedure. The stress field estimate was then updated to incorporate recent progress in statistical capabilities and new understanding of stress concentration factors for doorstopper cells, as well as to correct an error in the original stress solution procedure. Simple models were used to examine the possibility that systematic variations in material properties and stress fields existed at the site. These models succeeded in reducing the sum of squared error somewhat, but fell short of completely describing stress variations throughout the test site.

This overcore measurement will be supplemented by two other measurements described in the second and third reports of this series. Other observations of stress field characteristics are discussed in the fourth report. The final report will also characterize the natural in situ stress field in the vicinity of the Lucky Friday Mine. This work was undertaken to support USBM research on mining method design and rock-burst control for deep mines.

[1]Mining engineer, Spokane Research Center, U.S. Bureau of Mines, Spokane, WA.

INTRODUCTION

Researchers from the U.S. Bureau of Mines (USBM) undertook the investigations described in this report to increase basic knowledge of the in situ stress field at the Lucky Friday Mine in the Coeur d'Alene Mining District of northern Idaho. The study is based on an overcore stress measurement conducted by Allen (1979) in 1977 as part of a USBM study of mine shaft design in the Coeur d'Alene Mining District. Allen's stress measurement was chosen for review because the measurement site is conveniently located with respect to other USBM research projects in the Lucky Friday Mine, Mullan, ID. It also presented an opportunity to increase the accuracy of the analysis by applying recent advances in analytical capabilities, especially overcore stress concentration factors. As in situ stress measurements are very expensive to conduct, it was hoped that updating the analysis of this overcore measurement would be a cost-effective way to increase

basic knowledge of the district's in situ stress field. An update would also provide significant information for ongoing projects, which are aimed at developing improved mining methods and mitigating rock-burst hazards. Finally, the thorough description of the project in Allen's thesis and the availability of additional information, including detailed field notes, in USBM research files provided a good foundation for the review.

This report is the first in a four-part series that will examine the in situ stress field at the Lucky Friday Mine. The second report covers an overcore stress measurement conducted by USBM researchers on the 5300 level of the mine, and the third report describes a measurement on the 7300 level of the adjacent Star Mine. The final report examines observational evidence and characterizes the natural in situ stress field in the vicinity of the Lucky Friday Mine.

REVIEW OF AVAILABLE INFORMATION

Allen sought to measure the global in situ stress field in the vicinity of a proposed shaft. This objective required that the site be located far enough from mining to avoid mining-induced stress; however, cost considerations dictated that the site lie within existing mine openings. Furthermore, successful overcoring required competent rock that would provide intact diamond drill core samples where the instruments were to be placed. A site initially chosen on the 4450 level was abandoned when water inflow and highly fractured ground were encountered. The measurement location was then moved to an alternative site in an empty powder magazine just off the main haulageway on the 4250 level (figure 1). Ground conditions were better at the second site, but active mining was closer and more likely to affect stress measurements (figure 2). However, later investigations yielded a conservative estimate of mining-induced stress at the site at less than 15 pct of the maximum stress component (appendix A).

Geology at the site is complex, with the spine of a plunging anticline midway between boreholes 1 and 2. The anticline is made up of 0.3- to 2.5-cm (1/8- to 1-in) thick argillite seams between 2.5- to 30-cm (1- to 12-in) thick quartzite beds, which vary considerably in stiffness, strength, and brittleness. The quartzite also contains a small-scale depositional fabric, which has been shown to introduce a degree of strength and deformational anisotropy at some locations within the district (Whyatt, 1986). A test program to survey rock physical properties at the site was undertaken (appendix B).

OVERCORING PROCEDURES

Allen selected the biaxial strain cell developed by the Council for Scientific and Industrial Research, commonly known as a doorstopper cell, to use in obtaining overcore stress measurements. The difficulty in obtaining good core recovery at both the original and backup sites made this cell a particularly good choice. The doorstopper cell requires only about 8 cm (3 in) of 6-cm (2.375-in) diam core for a successful measurement (Jenkins and McKibbin, 1986) while alternative types of cells require longer and larger diameter core. During Allen's tests, the doorstopper cell overcoring procedure generally followed the manufacturer's recommendations. Although the cell has not been included in International Society for Rock Mechanics (ISRM) standard test procedures (1987) for overcore stress measurements, the procedure was generally consistent with recent ISRM guidelines for similar overcoring instruments (Gray and Toews, 1974).

The heart of the doorstopper cell is a four-element strain gauge rosette (figure 3) that is glued to the polished end of the borehole. An installation tool is used to center and orient the doorstopper cell on the end of the borehole. Temperature compensation is provided by a second doorstopper cell, housed inside the installation tool, that is glued to a similar piece of rock core.

In Allen's study, a set of readings was taken to establish a baseline strain state after the doorstopper cell glue set up and before overcoring. The installation tool and wiring

Figure 1

Test site

Borehole 2   Borehole 3

83

89

Borehole 1

82

65 ⊤

50

64

40 m

Vein

N

Scale, m

0   15   30

0   50   100

Scale, ft

KEY

- - - ↕ - - -   Fold axial plane

65 ⊤   Strike and dip of bedding
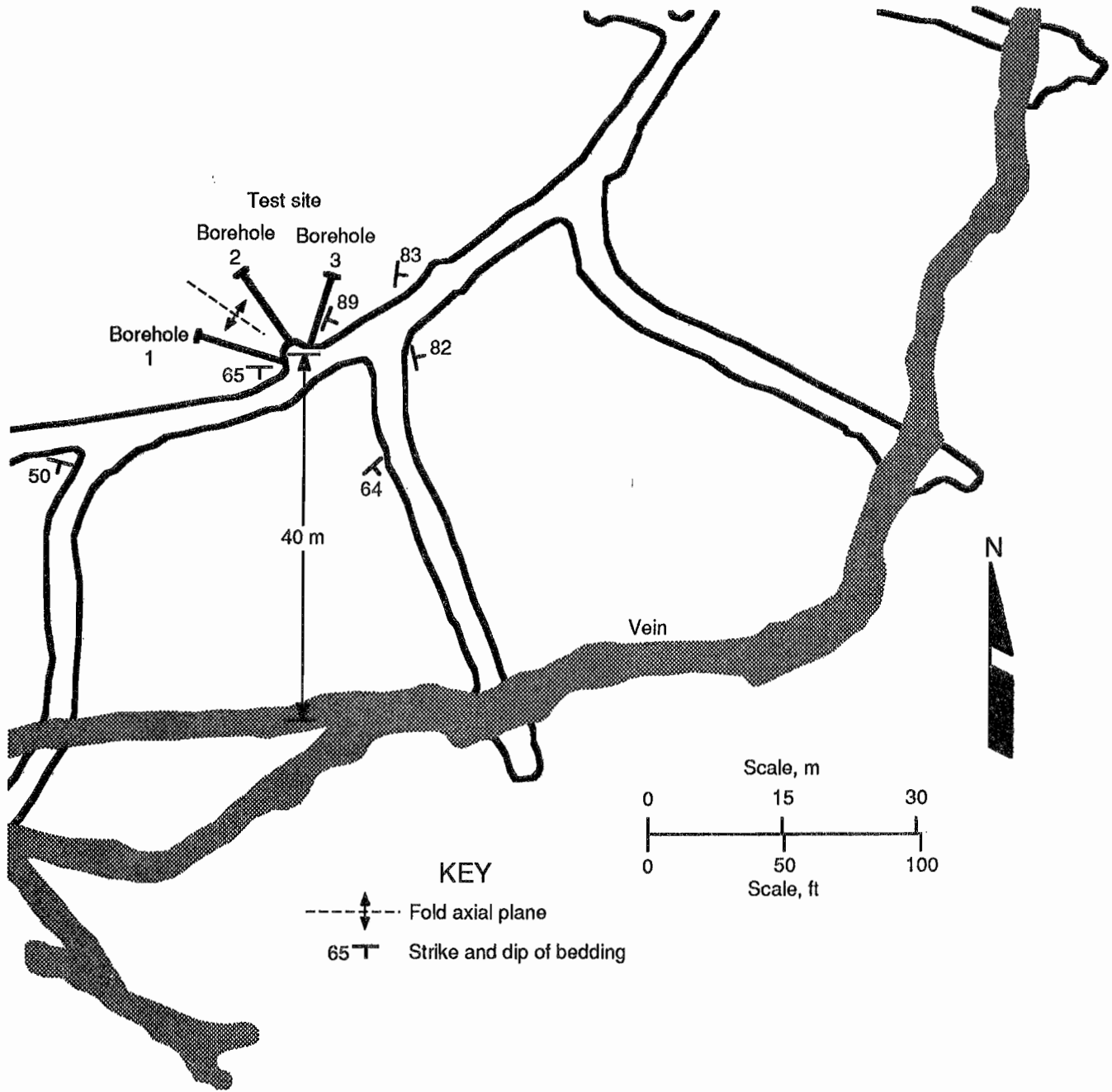
In situ stress measurement test site on 4250 level, Lucky Friday Mine.

Figure 2
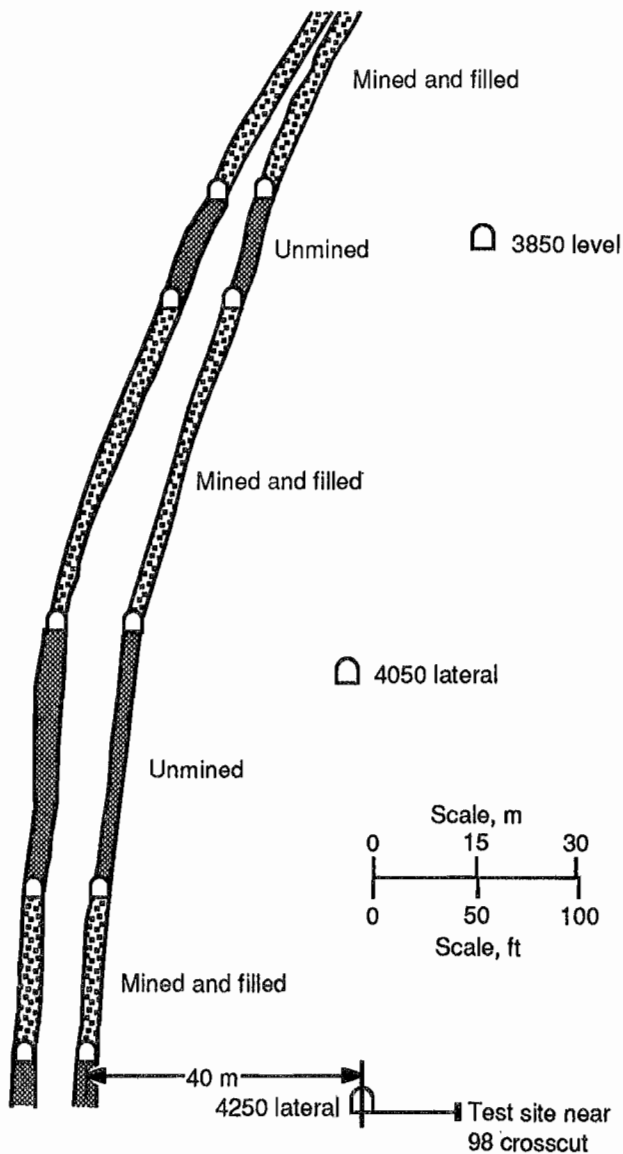
Vertical section view of test site.

then had to be removed to overcore the doorstopper cell. After extending the borehole with a diamond core bit (overcoring) about 8 cm (3 in) past the doorstopper cell, the installation tool was reattached to the doorstopper cell, and a number of final strain readings were taken for the destressed core.

Determination of a full three-dimensional, in situ stress state requires data from doorstopper cells in three non-parallel boreholes. However, the gauges are fairly inexpensive, so installing a large number of cells, like the 22 used in this project, is economically feasible. Overcoring

procedures have changed little since this measurement was completed, and a review of Allen's procedure and field notes encouraged confidence in the quality of his field measurements.

ORIGINAL DATA REDUCTION PROCEDURE

Allen was typical of early Coeur d'Alene district investigators in the treatment of data used to develop his in situ stress estimate. This was especially true with regard to his statistical treatment of data. The procedure he used is described in the remainder of this section.

Evaluation of Measurement Quality

Insight into the confidence Allen placed in each strain gauge can be obtained from two sources. The first is his field notes, which describe a number of problems encountered while installing and overcoring the doorstopper cells. The second is an examination of how he treated individual strain readings while developing his estimate of the in situ stress field. He discarded about one-eighth of the strain readings outright without reporting overcore strains. His notes for these measurements attributed failure to a number of problems, including difficulties with gluing the gauges to the end of the borehole, water fouling the gauges, and lapses in overcoring procedure.

Overcore strain readings were reported for the remaining 70 gauges, but only 28 (40 pct) of these readings were selected to develop the stress field estimate. Apparently, these gauges produced the overcore strain readings that Allen considered most reliable. These gauge readings are underlined in table 1 along with the specific difficulties he encountered during overcoring. Further excerpts from Allen's field notes are included as appendix C. As there appears to be some contradiction between the quality of strain readings suggested by the field notes and Allen's selection of strains in his in situ stress estimate, it would seem that other factors were considered, such as the elimination of overcore strains that appeared to be outliers. Between these two groups of overcore strain measurements was an intermediate group that Allen could not dismiss outright, but did not consider in his estimate of the in situ stress field.

Development of Strain Estimates for Each Gauge Orientation

Allen averaged selected overcore strains (underlined in table 1) to obtain the set of 12 average overcore strains shown in table 2 (one for each gauge orientation in each hole).

Figure 3

1.25–cm disk
of rock core

BX hole

Installation tool

Epoxy

Borehole
axis

Doorstopper cell

End of borehole

V

−45°   +45°

Doorstopper
cell

H

End of borehole

End view
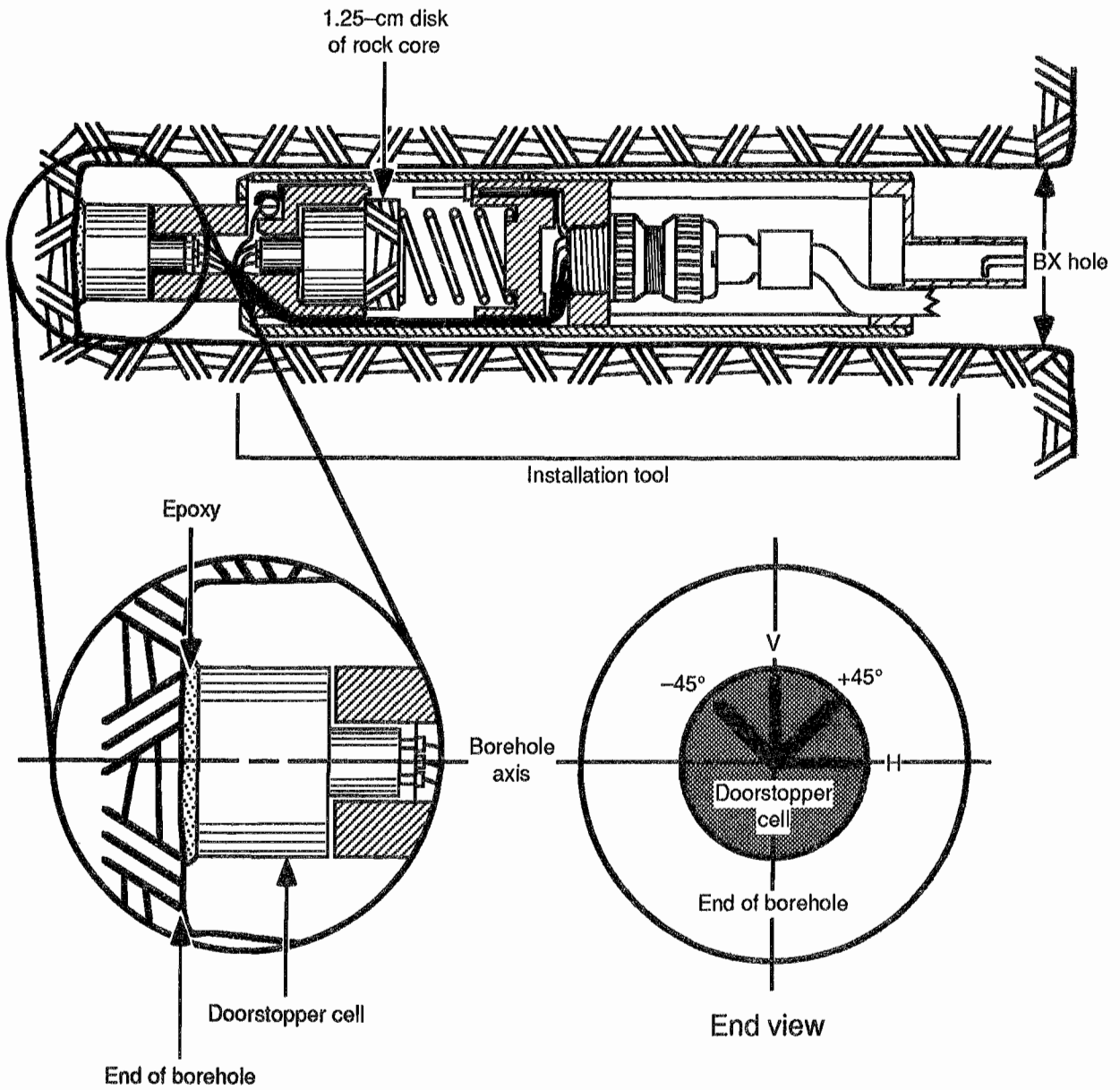
Schematic of doorstopper cell in borehole.

Table 1.—Summary of strain data from 4250-level site, microstrain

Doorstopper cell	Strain gauge orientation				Borehole depth		Notes
	+45°	-45°	Vertical	Horizontal			
Borehole 1:							
1	<u>713</u>	<u>565</u>	<u>226</u>	<u>1,064</u>	2.0 m	12 ft, 6 in	
2	<u>667</u>	300	<u>169</u>	<u>731</u>	4.7 m	15 ft, 6 in	
3	204	252	NM	314	6.4 m	21 ft	
4	240	<u>557</u>	.126	99	6.8 m	22 ft, 3 in	Bad glue bond.
5	NM	NM	NM	NM	7.3 m	24 ft	Argillite zone.
6	170	2,428	1,596	<u>768</u>	8.6 m	28 ft, 4 in	Electrical problems.
7	NM	NM	NM	NM	10.2 m	33 ft, 6 in	
8	<u>890</u>	<u>532</u>	400	71	10.6 m	34 ft, 9 in	Poor center, doorstopper worn by drill.
Borehole 2:							
9	562	510	101	<u>497</u>	3.7 m	12 ft, 3 in	
10	<u>658</u>	<u>566</u>	-51	<u>983</u>	5.9 m	19 ft, 4 in	Vertical fracture.
11	170	5	-73	113	6.9 m	22 ft, 7 in	
12	385	58	-33	<u>401</u>	7.5 m	24 ft, 7 in	
13	255	64	-168	<u>-347</u>	8.8 m	29 ft	
14	117	218	<u>135</u>	<u>170</u>	9.7 m	31 ft, 11 in	Polarity switch.
15	298	-368	-277	<u>275</u>	11.0 m	35 ft, 11 in	
Borehole 3:							
16	1,380	34	<u>533</u>	<u>1,080</u>	3.8 m	12 ft, 6 in	
17	<u>820</u>	<u>978</u>	<u>425</u>	NM	5.0 m	16 ft, 6 in	Bad glue bond.
18	1,112	<u>1,010</u>	1,993	747	7.5 m	24 ft, 6 in	Bad glue bond.
19	892	152	1,930	1,170	8.5 m	28 ft	
20	<u>650</u>	<u>747</u>	2,365	1,415	9.3 m	30 ft, 6 in	Highly fractured.

NM   Not meaningful.

NOTE.—Underlining indicates these strain readings were used in calculating mean strains shown in table 2.

Table 2.—Average strain readings calculated by Allen (1979)

Number of samples	Strain gauge orientation	Mean $\mu\epsilon$	Standard deviation
Borehole 1:			
3	- 45°	551	17.2
3	+45°	[1]757	11.8
3	Vertical	[1]251	13.9
3	Horizontal	[1]854	182.5
Borehole 2:			
1	- 45°	566	NM
1	+45°	658	NM
1	Vertical	[1]135	NM
5	Horizontal	[1,2]500	281.5
Borehole 3:			
2	- 45°	[2]912	93
3	+45°	[1]787	124
2	Vertical	[1]479	76
1	Horizontal	[1]1,080	NM

NM   Not meaningful.

[1]Mean strain used in stress solution.

[2]Allen changed sign of strain value from doorstopper 13 to obtain this mean.

Collection of Strain Components in Convenient Coordinate System

Allen selected a set of eight average overcore strains that lay in a single, convenient coordinate system and dismissed the rest. That is, while Allen selected overcore strain readings from -45° gauges in all boreholes and from +45° gauges in one borehole, he excluded them from the stress solution. The vertical overcore strain readings from each borehole were combined into a single, average, vertical overcore strain to reduce the set further, to the six overcore strain components presented in table 3. This rather arbitrary elimination of data appears to have been mandated by a stress solution program requirement that strain components lie at convenient orientations in a single Cartesian coordinate system and that the solution be exactly determined. The coordinate system was defined by the two outer and roughly horizontal holes, which represented the x- and y-axes, respectively, and an upward z-axis.

Table 3.—Selection and interpretation of strain measurements

Borehole	Strain gauge orientation	Average $\mu\epsilon$	Assumed strain component
1	Horizontal	854	ϵ_x
3	Horizontal	1,080	ϵ_y
1, 2, and 3 ..	Vertical	308	ϵ_z
2	Horizontal	500	[1]γ_{xy}
3	+45°	787	[1]γ_{yz}
1	+45°	757	[1]γ_{xz}

[1]This is a misdefinition of shear strain.

Unfortunately, Allen interpreted the last three overcore strains shown in table 3 as shear strains instead of viewing them as normal strains in a direction diagonal to the coordinate axes. In other words, Allen took the $+45°$ strain gauge data from the doorstopper cell as being shear strain on the face of the borehole. In fact, shear strain arises from normal strains according to the relationship

$$\gamma_{PR} = 2\epsilon_Q - \epsilon_P - \epsilon_R, \qquad (1)$$

where γ_{PR} = shear strain on the borehole face

and ϵ = normal strain measured by strain gauges in various orientations (shown in figure 4).

A complete development of strain components from a $45°$ strain gauge rosette like that used in a doorstopper cell can be found in most texts discussing experimental stress analysis (e.g., see Dalley and Riley, 1978). This misinterpretation undermined the validity of Allen's reported strain field and, as carried through the next two steps, the validity of his stress field estimate.

Calculation of Three-Dimensional Strain Tensor

The strain tensor follows exactly from a conveniently oriented set of six normal and shear strain components.

Calculation of Three-Dimensional Stress Tensor

The strain tensor (table 3) was converted to the stress tensor using Hooke's law and adjusted for the stress concentration effect at the end of the borehole. The modern description of the relationship between in situ stress and concentrated stress at the end of a borehole is given by equations 2 through 4 (Rahn, 1984).

$$s_{xx} = a\sigma_{xx} + b\sigma_{yy} + c\sigma_{zz}, \qquad (2)$$

$$s_{yy} = b\sigma_{xx} + a\sigma_{yy} + c\sigma_{zz}, \qquad (3)$$

and $$s_{xy} = (a - b)\sigma_{xy} = d\sigma_{xy}, \qquad (4)$$
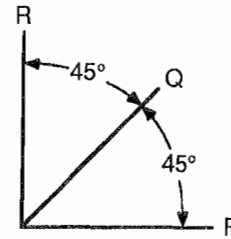
where s = stress on end of borehole,

$a, b, c,$ and d = constants,

σ = in situ stress field,

and $x, y,$ and z = coordinate axes.

The constants a, b, c, and d link the in situ stress field σ with the stress on the end of the borehole for a coordinate system with the z-axis parallel to the borehole axis. Allen reported using borehole stress concentration factors of a = d = 1.25 and b = c = 0, which he

Figure 4

Normal strain orientations used in equation 1.

attributed to an unpublished finite-element analysis by Chan.[2]

The theoretical basis for estimating the in situ stress field from doorstopper cell strain measurements has evolved considerably since the cell was introduced, and a number of sets of constants have been proposed since Allen conducted this work. Stress field estimates that result from various sets of constants are examined in appendix D.

Allen determined elastic properties for the stress estimate by laboratory tests on core samples from the three boreholes (appendix B). It is unclear what material properties were used; that is, Allen reported using a Young's modulus (E) of 56 GPa (8,100,000 psi) and a Poisson's ratio (ν) of 0.21, while Beus and Chan (1980) reported a Young's modulus of 52 GPa (7,500,000 psi) and a Poisson's ratio of 0.18. Both sources reported the same stress field. Examination of Allen's notes suggests that the subsequent publication by Beus and Chan is correct.

The resulting stress field estimate is presented in table 4. Although the estimate suffers from misdefinition of shear strain, the estimate still provides a direction for the maximum principal stress in line with other reported evidence (Whyatt, 1986), and an estimate of vertical stress reasonably close to Allen's estimate of 25 MPa (5,000 psi).

[2]Chan, S. S. M. Personal communication to Michael Allen, 1978.

Table 4.—In situ stress field at 4250-level site reported by Allen

Stress component	Magnitude		Bearing	Plunge
	GPa	psi		
σ_1	74	10,800	N 37° W	29°
σ_2	47	6,800	N 56° E	3°
σ_3	24	3,500	S 20° E	61°
σ_{H1}	62	9,000	N 40° W	
σ_{H2}	47	6,800	N 50° E	
σ_V	36	5,200		

NOTE.—Principal stresses are presented as reported by Allen (1979), and Beus and Chan (1980). An error in calculation of the secondary horizontal principal stress components (σ_{h1}, σ_{h2}) and vertical stress components (σ_v) has been corrected (after Whyatt, 1986).

STRESS FIELD ESTIMATE

An improved estimate of the in situ stress field relies on determining which of the many measurements from the doorstopper cell gauges are reliable and then applying statistical procedures and accurate stress concentration factors to minimize estimate error. Ideally, the rock mass at the site would be homogeneous and isotropic, and would lie far from the influence of mining. Such a stress field estimate would represent the far-field stress field that is loading mine openings.

EVALUATION OF STRAIN DATA

A reliable estimate of the in situ stress field depends on filtering out questionable overcore strain measurements that may distort the estimate. Allen, as noted previously, evaluated the quality of his measurements during overcoring and later, during development of his in situ stress estimate. A review of these two evaluations showed some apparent discrepancies. That is, readings from gauges that appeared to operate well in the field were later discarded when solving for the stress solution, while readings from gauges whose performance was questioned in the field were kept. This discrepancy may result from an attempt by Allen to eliminate outlier measurements, but this can not be documented. In any case, the importance of the selection process argues for further analysis of measurement quality. The analytical approach employed here checks to see if the doorstopper cells provide self-consistent strain readings.

The self-consistency of a doorstopper cell can be tested by determining whether all four strain gauges of a cell are measuring the same strain field (Gray and Toews, 1974). This so-called "strain test" takes advantage of the fact that any two perpendicular measurements of normal strain define the center of Mohr's circle in strain. Thus, each of two pairs of perpendicular gauges in a doorstopper cell should sum to the same total strain. If the sums are drastically different, the doorstopper cell is failing to measure a single strain field at the end of the borehole. This failure may be attributable to a number of factors, including an electrical problem, the presence of a fracture on or near the face, a poor or nonuniform glue joint, a change in rock properties from one gauge to the next, or improper centering of the cell. However, the strain test does not test for isotropic, elastic rock behavior.

A large difference between sums for a single cell indicates that the cell readings should be considered suspect in estimating the in situ stress field. However, definition

of "large" proved to be problematic. A rather arbitrary definition of large was chosen as being a difference greater than either $300 \ \mu\epsilon$ or 20 pct of the largest sum. This convenient cutoff eliminated over half of the cells but kept at least one cell in each hole. The strain test results are summarized in table 5.

While the strain test provides a convenient and purely quantitative measure of the confidence that may be placed in each strain measurement, the qualitative information on measurement accuracy provided by the field notes and Allen's selection of measurements is also valuable. This is especially true where one strain gauge in a cell failed, as occurred with doorstopper cells 3 and 17. Fortunately, considerable agreement was found between the field notes and results of the strain tests. However, there were some exceptions. In the case of doorstopper cells 13 and 19, no difficulties were mentioned in the field notes, but large discrepancies appeared in the strain tests. Therefore, readings from these two doorstopper cells were eliminated. Although doorstopper cell 6 showed good strain field results, electrical problems were noted during strain readings taken after overcoring, and a second set of readings taken after the cell was removed from the drill hole produced considerably different results (doorstopper cell measurement 6B in table 5). Thus, doorstopper cell 6 was also eliminated. In the two cases where a single gauge malfunctioned, cell 3 was selected and cell 17 rejected solely on the basis of Allen's notes. Thus, the screened data set is defined as that set that includes data from doorstopper cells 1 through 3 (except for the invalid gauge of 3), 12, 14, and 16 (see table 5).

The resulting overcore strain measurement data set is considerably different from Allen's. While Allen's data set included 27 measurements, and the current process selected 23 measurements, only 13 measurements were from both sets. This lack of overlap parallels the contradiction between field notes concerning measurement difficulties and Allen's selection of strain readings. A review of the measurements at issue suggests that Allen may have eliminated strains in order to reduce deviation from an average strain. While Allen's criteria for selecting measurements cannot be reconstructed, the selection of strain readings based on both field notes and strain tests appears to provide a satisfactory screening procedure for the available overcore measurements. Thus, the authors abandoned Allen's set of measurements in favor of this new set.

Table 5.—Doorstopper cell strain screening procedure, microstrain

Doorstopper cell	Strain gauge orientation				Strain test				Notes
	+45°	-45°	Vertical	Horizontal	Summation		Difference		
					±45°	H + V	µε	Pct	
Borehole 1:									
1*	713	565	226	1,064	1,278	1,290	12	1	(1)
2*	667	300	169	731	967	900	67	7	(1)
3*	204	252	NM	314	456				
4A	240	557	126	99	797	225	572	72	(2) Bad glue bond.
4B³	-240	557	126	99	317	225	92	29	(2) Bad glue bond.
6A	170	2,428	1,596	768	2,598	2,364	234	9	(1) Electrical problems.
6B³	280	1,564	424	172	1,844	596	1,248	68	(2)
8	890	532	400	71	1,422	471	951	67	(2) Doorstopper worn by drilling.
Borehole 2:									
9	562	510	101	497	1,072	598	474	48	(2)
10	658	566	-51	983	1,224	932	292	24	(2) Vertical fracture.
11	170	5	-73	113	175	40	135	77	(2)
12*	385	58	-33	401	443	368	75	17	(1)
13A	255	64	-168	-347	319	-515	834	162	(2)
13B³	263	75	-178	349	388	171	217	56	(2)
14*	117	218	135	170	335	305	30	9	(1) Polarity switch.
15	298	-368	-277	275	-70	-2	68	97	(2)
Borehole 3:									
16*	1,380	34	533	1,080	1,414	1,613	199	12	(1)
17	820	978	425	NM	1,798				Bad glue bond.
18	1,112	1,010	1,993	747	2,122	2,740	618	23	(2) Bad glue bond.
19	892	152	1,930	1,170	1,044	3,100	2,056	66	(2)
20	650	747	2,365	1,415	1,397	3,780	1,415	37	(2) Highly fractured.

H   Horizontal.
NM Not meaningful.
V   Vertical.
*   Selected for screened data set.
[1]Difference among strain sums was below limits.
[2]Difference among strain sums was above limits.
[3]Overcore strain reinterpretation (see appendix B).

NOTE.—Underlining indicates these strain readings were used in calculating mean strains shown in table 2.

REVISED STRESS FIELD SOLUTION

The conventional method of estimating in situ stress from overcore strain measurements develops a statistically optimum stress field that minimizes the squared error for each measurement. By treating all strain measurements from the test site equally, the site is assumed to have uniform rock properties and a homogeneous in situ stress field. A linear elastic rock mass with no discontinuities is also assumed. The personal computer (PC) program STRESsOUT (Larson, 1992) was used to develop stress field estimates based on this standard approach. STRESsOUT improved on Allen's method of solution by introducing

1. Statistical treatment of data. A least squares routine ensures equal (or specified) weighting of all data points.

2. Improved adjustments for borehole-induced stresses. Advanced modeling techniques have led to the development of more exact definitions of stress concentration factors on doorstopper cells. These definitions include the influence of Poisson's ratio on the induced stress field. The program allows the user to select from a number of reported stress concentration factors or supply the factors directly.

All stress estimates were developed with stress concentration factors provided by Rahn (1984) and physical properties reported by Beus and Chan (1980), i.e., E = 52 GPa (7,500,000 psi) and ν = 0.18. A number of data sets, including the new screened set, were used to develop the in situ stress field estimates shown in table 6. The full data set consists of data from all doorstoppers (table 5), using the alternative interpretations 4B, 6A, and 13B.

Table 6.—In situ stress estimates from data sets passing various screens and Allen's reported in situ stress estimate

Component	Magnitude		Bearing	Plunge
	MPa	psi		
Allen's reported in situ stress estimate:				
σ_1	74	10,800	N 37° W	29°
σ_2	47	6,800	N 56° E	3°
σ_3	24	3,500	S 20° E	61°
σ_v	36	5,200		
All data:				
σ_1	87	12,700	N 42° W	10°
σ_2	58	8,300	S 27° E	79°
σ_3	52	7,500	N 48° E	3°
σ_v	58	8,500		
Allen's selected strains:				
σ_1	103	14,900	S 34° E	9°
σ_2	62	9,000	S 58° W	16°
σ_3	60	8,700	N 26° E	72°
σ_v	61	8,900		
Screened data set (best estimate):				
σ_1	91	13,200	N 40° W	13°
σ_2	55	7,900	S 41° E	33°
σ_3	37	5,400	N 68° E	54°
σ_v	45	6,600		

These stress estimates differ considerably from Allen's reported estimate. The difference can be attributed, in part, to a combination of refinements in defining stress concentration factors and the availability of statistical procedures. The relative importance of these improvements is explored in appendix D.

In the new estimates, there is good similarity in maximum stress and maximum stress direction regardless of data set. However, estimates of the minimum principal stress (and the vertical stress component) vary widely. The screened data set developed in this investigation provides the best of these estimates and is presented in map coordinates in table 7.

Table 7.—Best estimate of stress field in map coordinates

Component	MPa	psi
σ_{ns}	74	10,700
σ_{ew}	64	9,200
σ_v	45	6,600
$\tau_{ns/ew}$	-19	-2,700
$\tau_{ew/v}$	-13	-1,900
$\tau_{v/ns}$	3	400

STRESS FIELD ASSUMPTIONS

After developing a best estimate of in situ stress through conventional means, it is appropriate to re-evaluate the underlying assumptions. These assumptions have been made for both the doorstopper cell and the measurement site.

DOORSTOPPER CELLS

The rock immediately surrounding a doorstopper cell is assumed to be homogeneous, continuous, isotropic, and linearly elastic. Uniaxial compression tests on core samples confirmed that the rock at this test site is reasonably linearly elastic, although some hysteresis at low loads is generally encountered. Since Allen inspected possible sites carefully with a rifle scope to avoid fractures and bed interfaces, the rock in the immediate vicinity of a doorstopper cell was probably homogeneous and continuous. This also suggests that the doorstopper cells were mounted inside the thicker beds. However, there would be no way to tell if a fracture lay just behind the end of the borehole, a condition that would distort the local stress field.

The presence of isotropic rock appears to be the most questionable assumption in the doorstopper cell analysis. In his description of core samples selected for a large number of Brazilian tests (appendix B), Allen noted bedding, presumably the fabric commonly observed within quartzite beds, in nearly all samples. It is quite likely that this bedding introduced some measure of anisotropy to the elastic behavior of the rock. Rahn (1984) and Amadei (1983) have developed the theoretical basis and stress concentration factors necessary for deducing stress in anisotropic rock. However, the available test information is not sufficient for estimating anisotropic elastic properties.

SITE

Assumptions about the measurement sites are particularly important when using two-dimensional gauges, which are incapable of measuring the entire stress tensor with a single cell. As can be seen from equations 2 and 3, the stress at the end of a borehole is significantly influenced by the stress component parallel to the borehole, which can be estimated from information provided by doorstopper cells in boreholes of other orientations. In fact, data from doorstopper cells in three nonparallel boreholes are needed to estimate the three-dimensional stress state. The least squares procedure followed in the previous section assumes that all doorstopper cells were installed in a homogeneous material in a homogeneous stress field. Any variations in material property or stress magnitude are considered random errors. Thus, averaging is used to give a best estimate of rock properties, and a

least squares algorithm is used to minimize error in estimating the in situ stress field.

However, if variations in material property or stress magnitude are real and not the result of random measurement error, a different approach is required. This is especially true if real variations occur in a systematic rather than an apparently random manner. Where systematic variations are understood, a model of site geologic structure and boundary conditions is essential for developing an understanding of the stress field at the test site.

The uniaxial compression tests conducted by Allen (appendix B) provide a good starting point for evaluating the distribution of material properties throughout the site. Figure 5 shows how the rock elastic modulus varies within

Figure 5
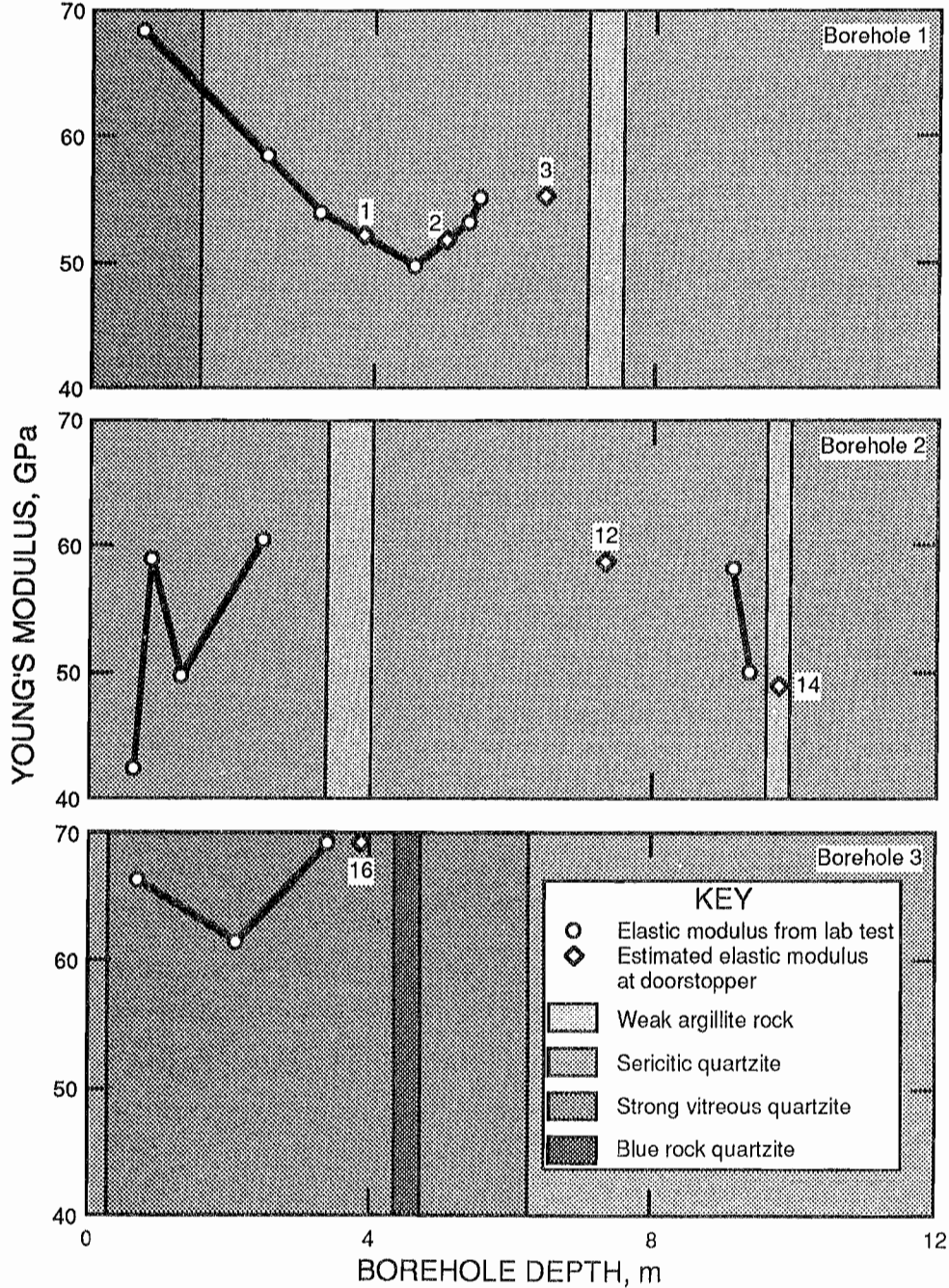
Variations in elastic modulus with borehole depth and doorstopper cell position. Stiff unit is deduced from bed orientation and elastic moduli. Elastic modulus for each doorstopper cell is extrapolated from test information (appendix A).

12

each borehole. These test results were combined with other sources of information, including the site geologic map (figure 1) and observations recorded in the drilling log (appendix C), to develop a geologic map of the test site (figure 6). Included in this map are estimates of the approximate position of hard and soft beds within the plunging anticline.

The strain field at the *end* of a borehole can be estimated from doorstopper cell strain readings (e.g., equation 1). The corresponding stress on the end of the borehole can easily be determined using Hooke's law (see Goodman, 1980, pp. 121-123, for a complete treatment). Local stress solutions, using average elastic properties, are presented in figures 7 through 9. These figures show the

Figure 6
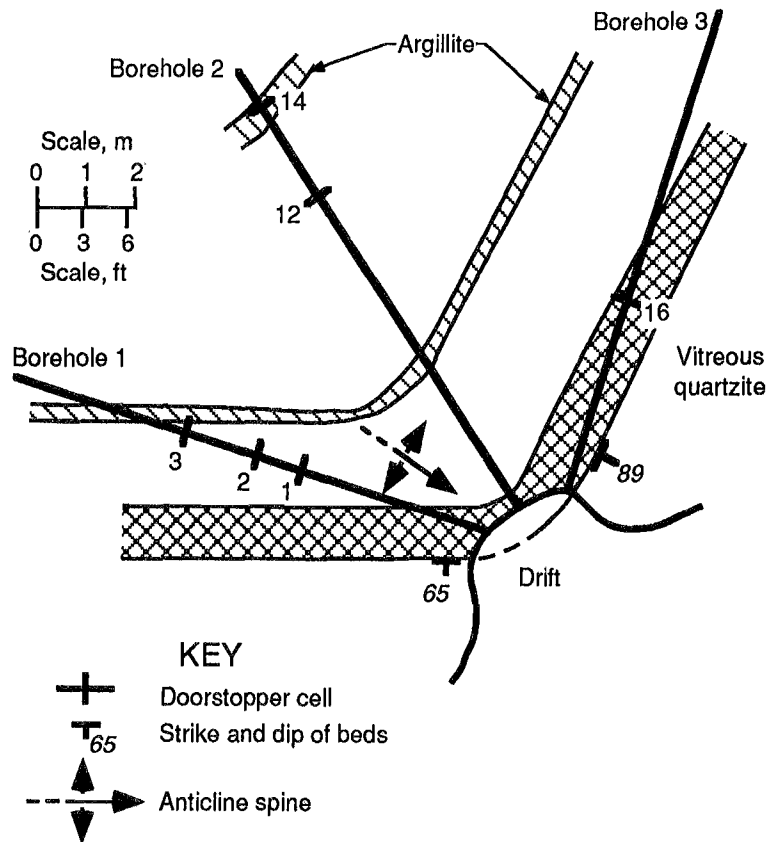
Anticline structure as determined from site map, drilling notes, and measured elastic moduli.

Figure 7

A

B

Argillite zone

③

③ — 6.1 m

②

② — 4.6 m

① — 3.0 m

① — 1.5 m

Scale, MPa

| 0 | 5 | 10 |

| 0 | 750 | 1,500 |

Scale, psi

65

Scale, m

| 0 | 1 | 2 |

| 0 | 3 | 6 |

Scale, ft

KEY

①   Doorstopper cell

T_{65} Strike and dip of beds
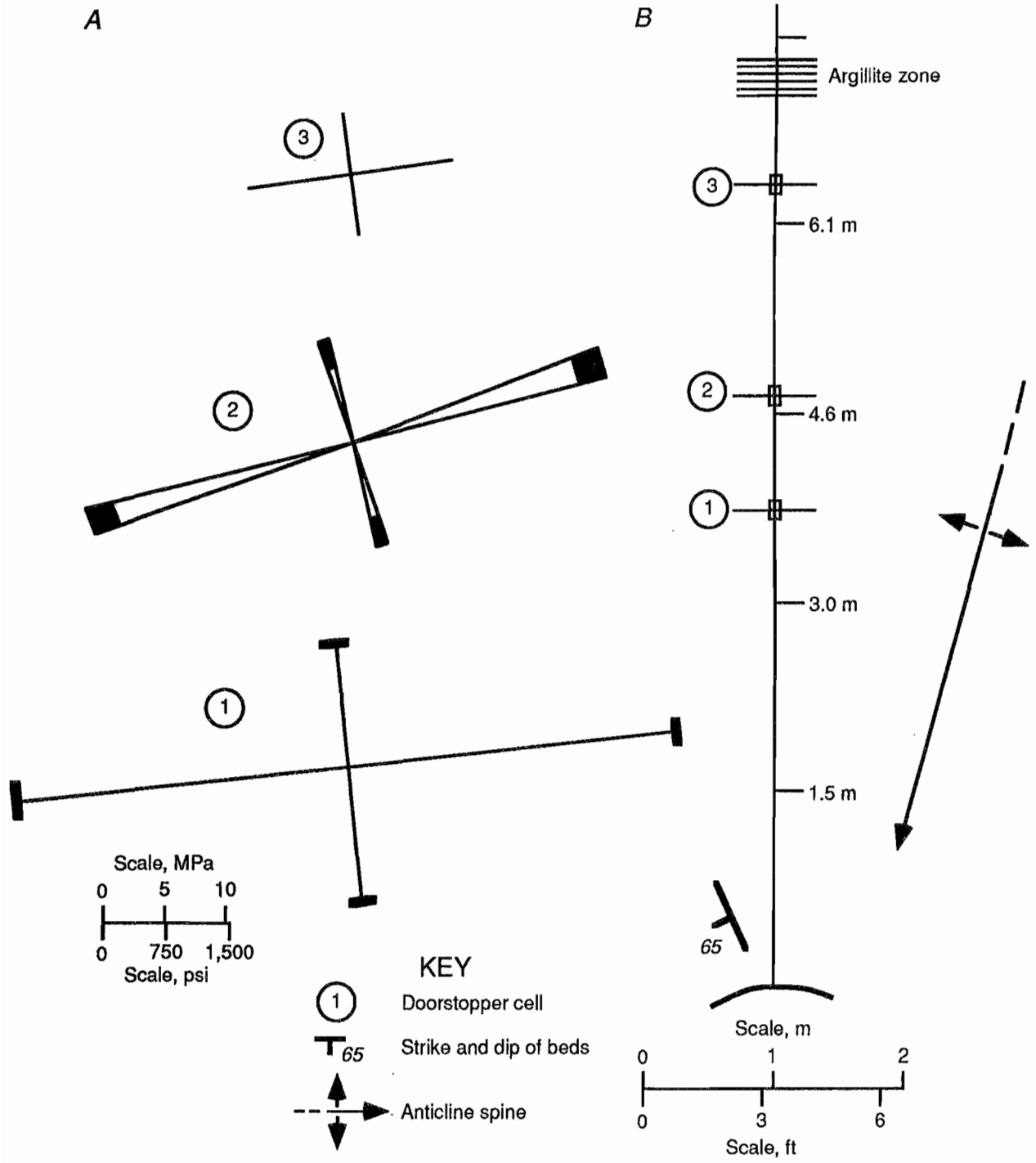
Anticline spine

Local stress and geology, borehole 1. A, Range of stress solutions for borehole using average elastic properties; B, borehole map and anticline spine.

Figure 8
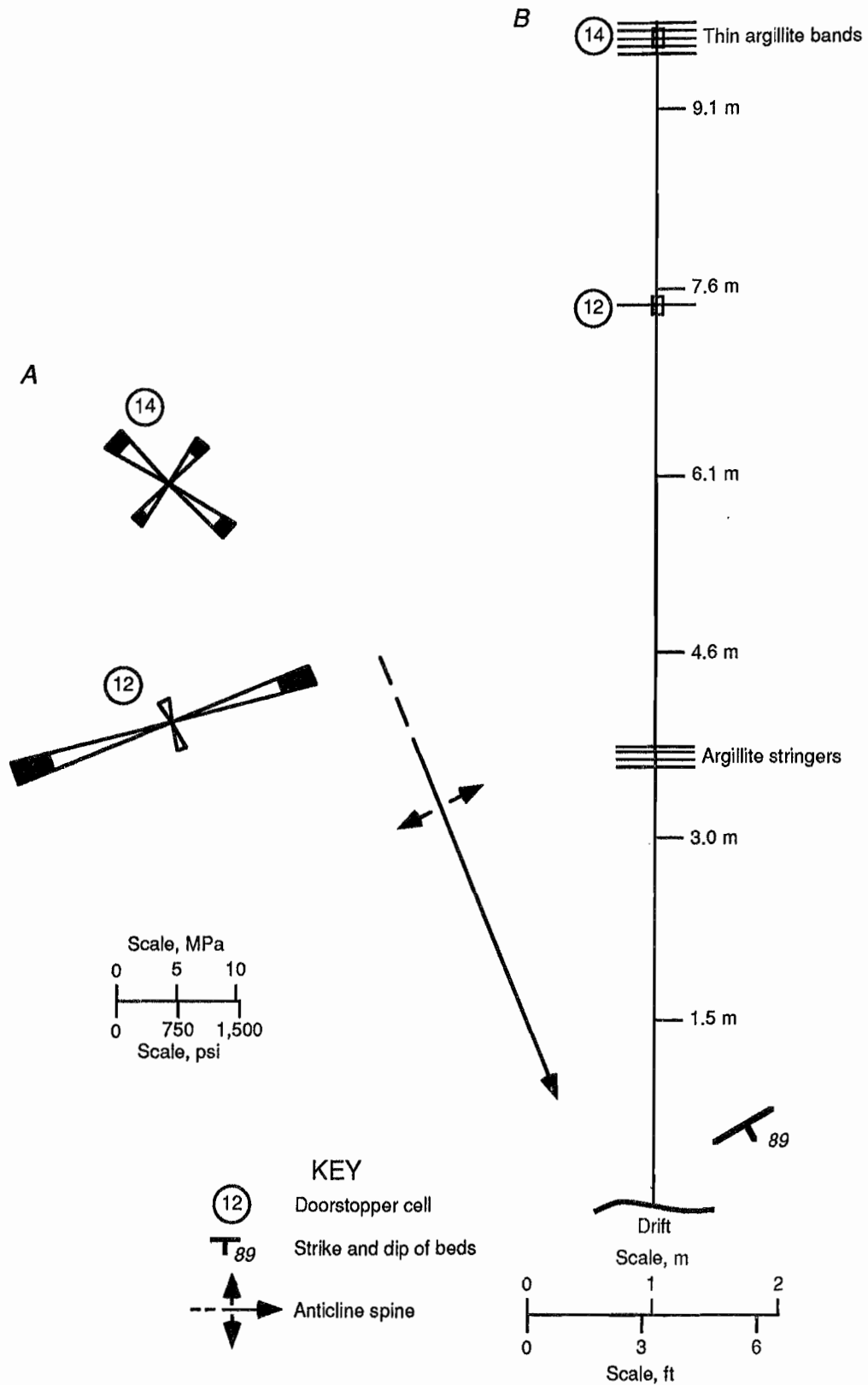
Local stress and geology, borehole 2. A, Range of stress solutions for borehole using average elastic properties; B, borehole map and anticline spine.

Figure 9

A

B

6.1 m

4.6 m

Silver and lead sulfides

3.0 m

Scale, MPa

0   5   10

0   750   1,500
Scale, psi

Scale, m

0   1   2

0   3   6
Scale, ft

1.5 m

KEY

(16)   Doorstopper cell

T_{89} Strike and dip of beds

- - - ▶   Anticline spine

89

Drift

Local stress and geology, borehole 3. A, Range of stress solutions for borehole using average elastic properties; B, borehole map and anticline spine.

range of stress solutions that result from using various combinations of three of the four doorstopper cell strain gauges. The stresses measured by doorstopper cells 1 and 2 in borehole 1 are fairly consistent, but the stress measured by cell 3 differs markedly in magnitude. Measurements from borehole 2 also show considerable variation.

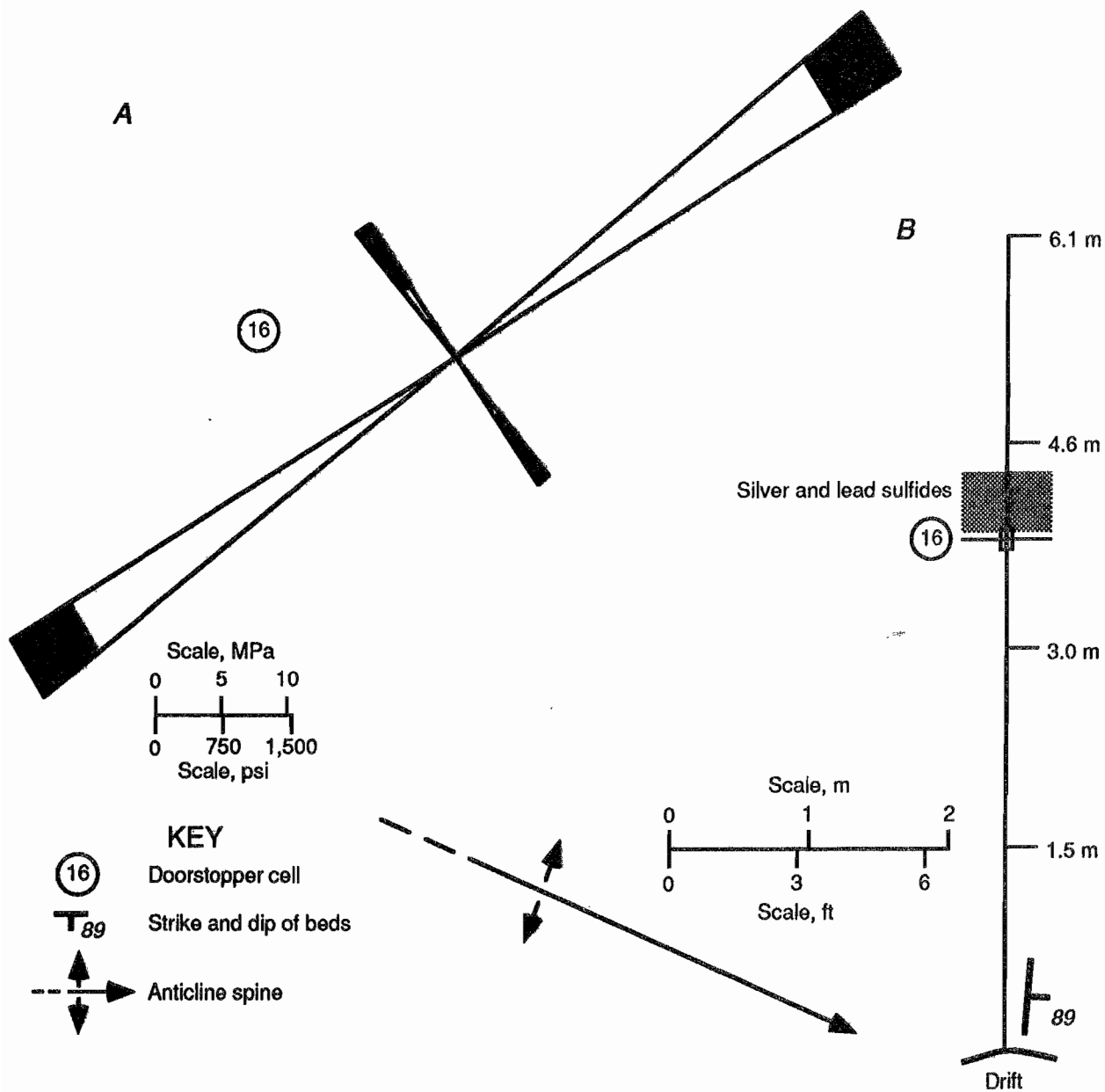These variations could be explained by any of a number of factors, including undetected experimental error, but the variation in rock properties among beds in the plunging anticline is probably the major factor. These figures also include available information on the orientation of bedding as measured at the borehole collar and geologic conditions within the boreholes noted during drilling.

ALTERNATIVE STRESS FIELD MODELS

The usefulness of a site model for developing an understanding of the in situ stress field is determined by the model's approximation of reality and its ease of application. The homogeneous, site-random error model assumed in conventional in situ stress measurements is easy to use. However, the complex geologic structure of the 4250-level test site departs significantly from the homogeneous model. Modern numerical modeling programs can produce a wide range of stress field models based on various assumptions for load history, past inelastic deformation, boundary conditions, rock properties between measurement points, and joint properties. However, such a procedure is not easy to use and depends on parameters that are difficult to measure or even estimate.

Introducing a useful alternative model of the stress field depends on ensuring that the added complexity of the model is fully supported by available information and that this complexity can be integrated into stress estimation routines in a convenient manner. If the information required by a stress model outstrips that available from the field, the uncertainties associated with assuming unknowns can quickly negate the insight gained by departing from the conventional model. The success or failure of simple models in improving the fit to measured overcore strains provides added insight into the dominant characteristics of the stress field. This information can be used to "bootstrap" the analysis to models of greater detail in the manner outlined by Starfield and Cundall (1988). However, the uniqueness of a successful model cannot be assured. That is, more than one model may produce reasonable local stresses at each doorstopper cell.

Two simple alternative models are proposed that modify the conventional model to take into account the variation of rock elastic modulus through the test site. The simplicity of these models introduces some physical inconsistencies, but they should show whether modification of the analysis model can improve the result.

CONSTANT STRESS MODEL

This model assumes that a constant stress field exists throughout the rock mass along with real variations in elastic modulus. That is, stiffer regions of the rock mass carry the same load as softer regions. It is difficult to imagine the physical mechanisms that might generate such a stress field. However, this model may provide a closer approximation to reality than the conventional model, which ignores variations in both elastic modulus and in situ stress.

The constant stress model can be introduced into the solution process by adjusting each doorstopper cell for local elastic modulus. Since STRESsOUT does not allow specification of elastic modulus for individual cells, overcore strain measurements were adjusted through multiplication with the ratio of local-to-site moduli. For example, rock near doorstopper 16 had an estimated modulus of 69 GPa (10,000,000 psi), producing a strain-adjustment ratio of 1.33 [69:52 GPa (10,000,000:7,500,000 psi)]. This way, a cell in stiff rock reports higher stress levels than a cell in soft rock for similar overcore strains. Application of this adjustment to the screened data set produced the in situ stress estimate shown in table 8.

Table 8.—Stress field estimate using constant stress-variable modulus model

Stress component	Magnitude		Bearing	Plunge
	MPa	psi		
σ_1	112	16,200	N 45° W	15°
σ_2	64	9,200	S 36° W	30°
σ_3	44	6,400	N 68° E	56°
σ_v	54	7,800		

CONSTANT STRAIN MODEL

This model assumes that a constant strain field exists throughout the rock mass along with real variations in elastic modulus. This is a simple way to allow for variation of both stress and elastic modulus without having to resort to a detailed numerical model of the site. It is difficult to imagine the physical mechanisms that might give rise to this model. However, this model may provide a closer approximation to reality than the conventional model, which ignores variations in both elastic modulus and in situ stress.

The constant strain model is easily integrated into STRESsOUT calculations. The procedure is fairly simple. First, the conventional solution is taken from table 6. This solution is simply Hooke's law applied to the constant strain field solution. Local stresses can be estimated by adjusting for the local elastic modulus. For example, the stress solution is modified to estimate the stress field near doorstopper 16 by multiplying by the ratio of local to average elastic moduli of 1.33 [69:52 GPa (1,000,000:7,500,000 psi)].

SITE MODEL VALIDATION

The fidelity of the conventional and proposed alternative models to reality can only be evaluated against real measurements. The vertical component of stress, which is sampled by all of the doorstoppers, is an obvious candidate. Calculation of the in situ vertical stress component would require knowledge of the stress parallel to the borehole, information not available from the doorstopper cell. However, the vertical stress on the *end* of the borehole can be found from the information provided by a single doorstopper and can also be calculated from in situ stress estimates derived using the various models. These measured values were included in the individual cell plots and are tabulated in table 9 and summarized in figure 10. Values calculated from each of the three analytic models are also included in table 9. The sum of squared error was calculated for each model.

Table 9 shows that the constant stress and constant strain models have a lower squared error than the conventional model for the vertical strain component. The nearly 30-pct reduction in squared error attained by the constant strain (and variable stress) model suggests that there may be real stress variations at the site. The constant strain model has the greatest error in its estimate for doorstoppers 1 and 16, which had the greatest local vertical stress measurements.

In situ horizontal and vertical stress at each doorstopper cell can be estimated by assuming that the best estimate of stress (table 6) provides a reasonable estimate of the stress component parallel to each borehole The in situ vertical stress components illustrated in figures 11 and 12 were estimated on this basis. The results show stress to be roughly proportional to elastic modulus, as would be the case for the constant strain model.

Table 9.—Predicted versus measured vertical stress on end of borehole

Doorstopper	Measured stress		Conventional model		Constant stress		Constant strain	
	MPa	psi	MPa	psi	MPa	psi	MPa	psi
CONCENTRATED VERTICAL STRESS COMPONENT								
1	23.5	3,412	10.3	1,489	8.7	1,256	10.3	1,489
2	17.6	2,550	10.3	1,489	8.7	1,256	10.3	1,489
3	11.8	1,704	10.3	1,489	8.7	1,256	11.0	1,588
12	4.1	595	4.9	706	3.5	501	5.5	800
14	10.9	1,575	4.9	706	3.5	501	4.5	659
16	52.4	7,600	21.0	3,039	26.0	3,769	27.9	4,052
MODEL ERROR (MEASURED STRESS MINUS MODEL STRESS)								
1			13.3	1,923	14.9	2,156	13.3	1,923
2			7.3	1,061	8.9	1,294	7.3	1,061
3			1.5	215	3.1	448	0.8	116
12			-0.8	-111	0.7	94	-1.4	-205
14			6.0	869	7.4	1,074	6.3	916
16			31.0	4,561	26.4	3,831	24.5	3,548
Sum of squared error × 10^6			0.18		0.15		0.13	

Figure 10
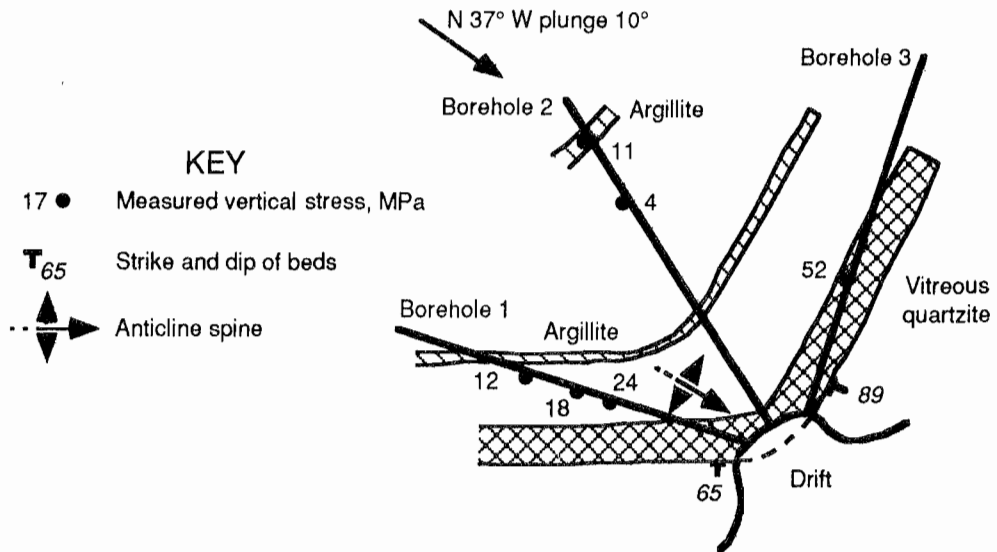
Vertical stress component on end of borehole as estimated for selected doorstopper cells. Estimates are based on single doorstopper cell solutions and moduli from figure 5. Note high stress in vitreous quartzite. The preexisting vertical stress at each doorstopper depends on magnitude of stress component parallel to each borehole.

Figure 11
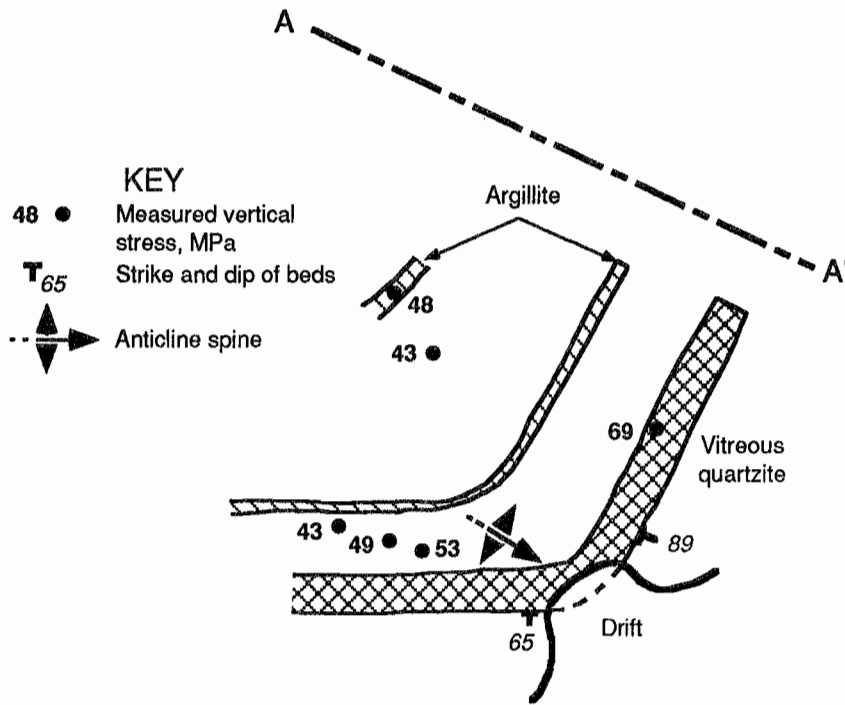
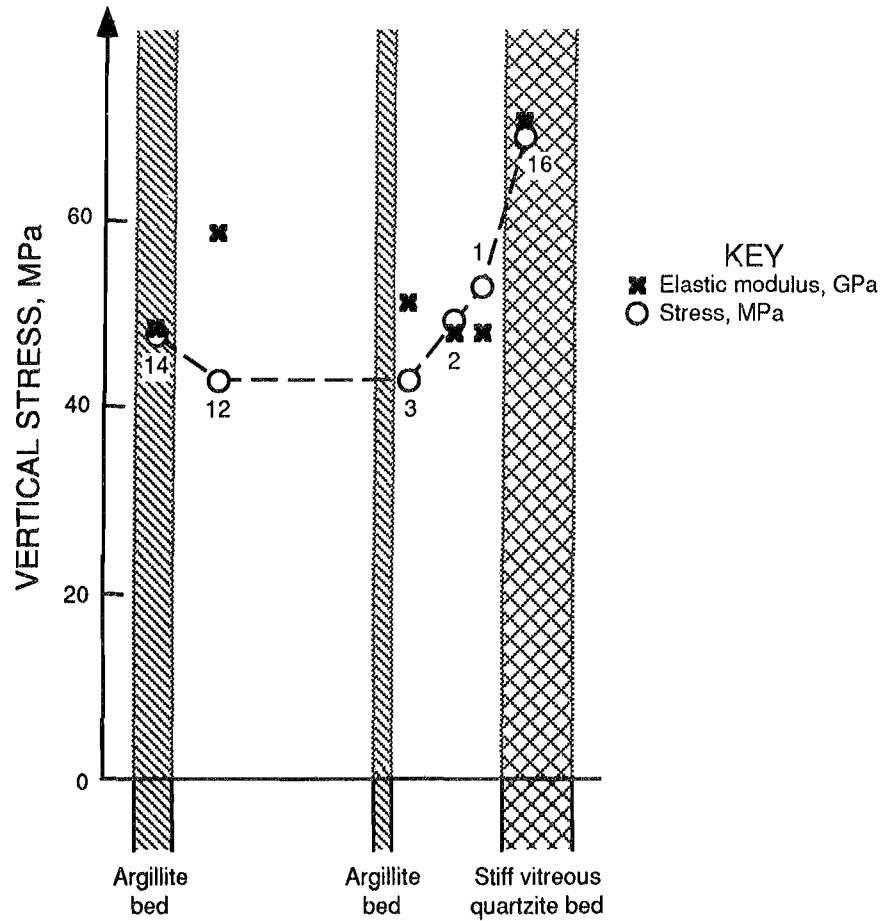*Plot of estimated vertical in situ stress components by doorstopper location.*

Figure 12

Plot showing relationship among stratigraphy, rock elastic modulus, and esti-
mated vertical in situ stress component. Numbers indicate doorstopper cells.
Both doorstopper cells and elastic modulus (heavy crosses) are plotted as to
relative stratigraphic position. Note that elastic modulus is read as GPa, while
vertical stress is read as MPa.

DISCUSSION AND CONCLUSIONS

A critical review of Allen's measurement of stress on
the 4250 level of the Lucky Friday Mine found that his
field measurements of overcore strain were reliable. How-
ever, a review of the reported stress solution revealed
several deficiencies, including poor estimates of door-
stopper cell stress concentration factors, no statistical
treatment of the data, and misdefinition of shear strain.
A new estimate of in situ stress at the site was developed
using the assumption that all deviations in measurements
of rock elastic modulus and overcoring strain were the
result of random error.

An examination of geologic information and the dis-
tribution of measured elastic moduli from the three bore-
holes suggested that material properties were distributed
systematically in the beds of the steeply plunging anticline
at the site. Furthermore, vertical stress appears to vary
systematically in a similar manner.

Simple models that recognized variation of material
properties through the site were proposed and used to de-
velop alternative solutions. These solutions did succeed in
reducing the sum of the squared error produced by pre-
dicting the vertical stress measured by each doorstopper

cell. Further improvements might be realized with a detailed three-dimensional structural model of the site.

Planning for future overcore stress measurements in the Lucky Friday Mine, and in other mines with complex geologic settings, should anticipate the possibility that systematic variations in material properties and stress fields exist at the test site, as well as the presence of elastic anisotropy. In such cases, thorough geologic mapping, core logging, and laboratory testing must be included in the measurement program. In addition, methods are needed to ensure unbiased sampling and to integrate the stress field estimation procedure with detailed models of site heterogeneities.

ACKNOWLEDGMENTS

REFERENCES

Allen, M. Determining the In-Situ Stress Field on the 4250 Level in the Lucky Friday Mine: Using the CSIR Biaxial Strain Gage and Structural Geologic Mapping. M.S. Thesis, Univ. ID, Moscow, ID, 1979, 73 pp.

Amadei, B. Rock Anisotropy and the Theory of Stress Measurements. V. 2: Lecture Notes in Engineering, ed. by C. A. Brebbia and S. A. Orzag. Springer-Verlag, NY, 1983, 478 pp.

Beus, M. J., and S. S. M. Chan. Shaft Design in the Coeur d'Alene Mining District—Results of In Situ Stress and Physical Property Measurements. USBM RI 8435, 1980, 39 pp.

Bonnechere, F. A., and C. Fairhurst. Determination of Regional Stress Field from "Doorstopper" Measurements. Ch. in International Symposium on the Determination of Stresses in Rock Masses (Proc., Lisbon, Portugal, 1969). Nat. Lab. of Civil Eng., Lisbon, Portugal, 1971, pp. 307-333.

Corson, D. R., and W. R. Wayment. Load-Displacement Measurement in a Backfilled Stope of a Deep Vein Mine. USBM RI 7038, 1967, 51 pp.

Dalley, J. W., and W. F. Riley. Experimental Stress Analysis. McGraw-Hill, NY, NY, 2d ed., 1978, pp. 318-333.

Goodman, R. E. Introduction to Rock Mechanics. Wiley & Sons, NY, NY, 1980, 478 pp.

Gray, W. M., and N. A. Toews. Optimization of the Design and Use of a Triaxial Strain Cell for Stress Determination. ASTM STP 154, 1974, pp. 116-134.

Hocking, G. Three-Dimensional Elastic Stress Distribution Around the Flat End of a Cylindrical Cavity. Int. J. of Rock Mech., Min. Sci., & Geomech. Abstr., v. 13, 1976, pp. 331-337.

International Society for Rock Mechanics. Suggested Methods for Rock Stress Determination. Int. J. Rock Mech. Min. Sci. & Geomech. Abstr., v. 24, No. 1, 1987, pp. 53-74.

Jenkins, M., and R. McKibbin. Practical Considerations of In Situ Stress Determination. Ch. in Proceedings, International Symposium on Application of Rock Characterization Techniques in Mine Design, ed. by M. Karmis. Soc. Min. Eng. (Littleton, CO), 1986, pp. 33-39.

Larson, M. K. STRESsOUT—A Data Reduction Program for Inferring Stress State of Rock Having Isotropic Material Properties: A User's Manual. USBM IC 9302, 1992, 158 pp.

Leijon, B. A. Relevance of Pointwise Rock Stress Measurements - An Analysis of Overcoring Data. Int. J. Rock Mech. Min. Sci. & Geomech. Abstr., v. 26, No. 1, 1989, pp. 61-68.

Pariseau, W. G., J. K. Whyatt, and T. J. McMahon. Rock Mechanics Investigations at the Lucky Friday Mine (In Three Parts): 3. Calibration and Validation of a Stope-Scale, Finite-Element Model. USBM RI 9434, 1992, 16 pp.

Rahn, W. Stress Concentration Factor for the Interpolation of "Doorstopper" Stress Measurements in Anisotropic Rocks. Int. J. Rock Mech. Min. Sci. & Geomech. Abstr., v. 21, No. 6, 1984, pp. 313-326.

Starfield, A. M., and P. A. Cundall. Towards a Methodology for Rock Mechanics Modeling. Int. J. Rock Mech. Min. Sci. & Geomech. Abstr., v. 25, No. 3, 1988, pp. 99-106.

Van Heerden, E. W. Stress Concentration Factors for the Flat Borehole End for Use in Rock Stress Measurements. Eng. Geol., v. 3, 1969, pp. 307-323.

Whyatt, J. K. Geomechanics of the Caladay Shaft. M.S. Thesis, Univ. ID, Moscow, ID, 1986, 195 pp.

Whyatt, J. K., T. J. Williams, and M. P. Board. Rock Mechanics Investigations at the Lucky Friday Mine (In Three Parts): 2. Evaluation of Underhand Backfill Practice for Rock Burst Control. USBM RI 9433, 1992, 10 pp.

APPENDIX A.—MINING-INDUCED STRESS AT OVERCORE SITE

The level of mining-induced stress at the measurement site was estimated with a MINSIM-D boundary element model of the Lucky Friday Mine. Model runs conducted with and without backfill estimated the mining-induced stresses presented in table A-1. The magnitudes of mining-induced stress components are less than 15 pct of horizontal in situ stress levels. Thus, mining-induced stress should not have a major influence on the measured in situ stress. Backfill does not appear to have an effect on mining-induced stress at the measurement site.

A uniform, elastic rock mass was assumed. The rock mass modulus was softened from laboratory values to match the model calibration reported by Pariseau, Whyatt, and McMahon (1992). Backfill properties were estimated based on the work of Whyatt, Williams, and Board (1992), and Corson and Wayment (1967). Yearly excavation steps were used to place and load backfill. Fill properties were adjusted for the yearly timesteps and fit to stope closures of up to 30 pct. Larger closure magnitudes are not evident at the Lucky Friday Mine. Rock mass and fill properties used in the model are summarized in table A-2.

Table A-1.—Mining-induced stress at measurement site

Component	In situ stress		Mining-induced stress without backfill		Mining-induced stress with backfill	
	MPa	psi	MPa	psi	MPa	psi
σ_{xx}	69.93	10,100	6.32	920	4.22	610
σ_{yy}	69.93	10,100	-0.97	-140	-1.10	-160
σ_{zz}	34.97	5,050	-4.32	-630	-4.91	-710
τ_{xy}	0.0	0	1.96	280	1.56	230
τ_{yz}	0.0	0	8.40	1,220	7.14	1,040
τ_{zx}	0.0	0	10.81	1,570	9.60	1,390

NOTE.—Compressive strength is positive.

Table A-2.—Rock mass and fill properties used in estimating mining-induced stress

Rock mass properties:	
Elastic modulus, GPa	70
Poisson's ratio	0.2
Fill shear strength:	
Cohesion, MPa	0
Friction angle	20°
Fill normal stiffness:[1]	
First load constant, a, MPa	-69,000
Ultimate strain, b	50
Second load constant, c, MPa	70,000
Transition strain, ϵ_t	0.05

[1]Fill behavior is defined as nonlinear spring according to the following equation:

$$P = \frac{c\epsilon^2}{b - \epsilon}$$

and

$$P = \frac{a(\epsilon - \epsilon_t)^2 + c\epsilon^2}{b - \epsilon},$$

where P = wall-to-wall fill pressure,

         ϵ = fill strain,

and ϵ_t = transition strain, m/m.

APPENDIX B.—RESULTS OF PHYSICAL PROPERTY TESTS

Table B-1.—Average rock properties

Description	No. of samples	Mean			Standard deviation		
		GPa	MPa	psi	GPa	MPa	psi
UNIAXIAL COMPRESSION[1]							
Borehole 1:							
Young's modulus	6	53		8,200,000	7.6		840,000
Strength	4		280	42,000		25	4,500
Borehole 2:							
Young's modulus	6	53					
Strength	4		320	7,700,000	7.2		950,000
Borehole 3:				47,000		37	4,700
Young's modulus	3	65					
Strength	3		450	9,400,000	4.1		490,000
				65,000		30 ·	3,500
Av. Young's modulus ..	13	56		8,200,000	7.2		1,040,000
INDIRECT TENSION[2]							
Loads on perpendicular beds ..	10		18	2,653		1.3	191
Loads on parallel beds	20		8.7	1,261		3.0	439
TRIAXIAL[2,3]							
Boreholes 1 and 2:							
σ_3 = 69 MPa (1,000 psi)	2		392	56,800		29	4,242
σ_3 = 138 MPa (2,000 psi) ...	2		451	65,400		37	5,374
σ_3 = 276 MPa (4,000 psi) ...	2		717	104,000		47	6,788
Borehole 3:							
σ_3 = 69 MPa (1,000 psi)	2		790	114,600		15	2,242
σ_3 = 138 MPa (2,000 psi) ...	1		1,100	159,600		NAp	NAp
σ_3 = 276 MPa (4,000 psi) ...	2		1,116	161,800		53	7,636

NAp   Not applicalble.

[1]Statistics calculated from table B-3. These values differ from those reported by Allen, but the source of the difference is not apparent from the available information.

[2]Statistics as reported by Allen.

[3]Allen notes that "Physical rock properties for holes 1 and 2 differ substantially from hole 3. This difference is due to the occurrence of the 'blue rock' variety of Revett Quartzite in which the third hole was drilled."

Table B-2.—Poisson's ratio[1]

Borehole	Number of samples	Mean	Standard deviation
1	6	0.21	0.07
2	6	0.22	0.12
3	2	0.30	0.16
Average	12	0.23	0.11

[1]Statistics calculated from table B-3.

Table B-3.—Results from individual compression tests

Borehole	Young's modulus		υ	Strength		Borehole depth	
	GPa	10^6 psi		MPa	psi		
1	68	9.9	0.22	262	37,977	0.8 m	2 ft, 6 in
	59	8.5	0.18	336	48,700	2.4 m	8 ft
	54	7.8	0.15	NA	NA	3.2 m	10 ft, 6 in
	50	7.3	0.15	263	38,200	5.6 m	15 ft
	53	7.7	0.36	299	43,400	5.3 m	17 ft, 6 in
	55	8.0	0.22	NA	NA	5.5 m	18 ft
2	42	6.1	0.15	352	51,000	0.6 m	2 ft
	59	8.6	0.21	359	52,000	0.8 m	2 ft, 6 in
	50	7.2	0.21	NA	NA	1.2 m	4 ft
	60	8.7	0.46	305	44,200	2.4 m	7 ft, 10 in
	58	8.4	0.26	281	40,700	9.0 m	29 ft, 6 in
	49	7.2	0.08	NA	NA	9.1 m	30 ft
3	66	9.5	0.14	471	68,300	1.1 m	3 ft, 6 in
	61	8.8	4.60	415	60,200	2.0 m	6 ft, 8 in
	69	10.0	NA	460	66,700	3.3 m	10 ft, 8 in

NA   Not available.

υ = Poisson's ratio.

Table B-4.—Elastic modulus extrapolated for selected doorstopper cells

Doorstopper	GPa	psi
1	52	7,500,000
2	52	7,500,000
3	55	8,000,000
12[1]	59	8,500,000
14[2]	48	7,000,000
16	69	10,000,000

[1]Sample appears to be from the center of a competent zone.

[2]Thin argillite beds appear to reduce modulus both directly and by associated increases in argillite in surrounding quartzite. As core recovery in argillite is almost impossible, the doorstopper cell is probably in quartzite.

APPENDIX C.—OVERCORE FIELD NOTES AND INTERPRETATION

This appendix presents field notes available from the overcores from each doorstopper cell. The authors' comments are added in brackets. Notes from cells 19 and 20, borehole 3, were not available.

Hole No. 1: Azimuth: 287°, Inclination: -5°

Doorstopper No. 1   Depth 12'6"

The original core was 6" long, two parallel fractures split the core into three equal sections. The fractures are approx. 30° from horizontal. The fractures appear to have been secondary features in the rock which were hairline.... [Unreadable]

Doorstopper No. 2   Depth 15'6"

Good bond, pure quartzite, fracture appears to be caused by drilling.

Doorstopper No. 3   Depth 21'0"

No initial vertical readings were taken due to V channel not operating. Good bond, fracture due to drilling.

Doorstopper No. 4   Depth 22'3"

Poor bonding, too much epoxy, quartzite doorstopper broke off core after obtaining final readings. [Allen used channel 45+ = 240 $\mu\epsilon$, apparently assuming a polarity error in wiring. However, 45+ = -240 $\mu\epsilon$ is indicated by field notes and performs better in the screening process. See the overcore strain plot of figure C-1A.]

Doorstopper No. 5   Depth 24'0"

No final data was obtained for this doorstopper. The doorstopper broke off before we could obtain the final readings.

Argillic quartzite. The doorstopper was epoxyed on a 5" argillic quartzite core, with a fracture plane located 1" from the doorstopper. The fracture was filled in with talc and appeared to be the contact between the argillic quartzite and a argillic stringer.

Doorstopper No. 6   Depth 28'4"

Good bond, pure quartzite fracture due to drilling. Water problems in the hole may have affected some channels. [A later reading was taken after the doorstopper was removed from the borehole. This is presented as the second measurement from doorstopper 6 in table 5.]

Doorstopper No. 7   Depth 33'6"

No data was obtained for this doorstopper. A 3" piece of core was still in the hole when the doorstopper was installed.

Doorstopper No. 8   Depth 34'9"

Good bond on argillaceous qtzite with vertical fracture 1/4" behind doorstopper. Old fracture and some vertical parting. A portion of the doorstopper was slightly worn by drilling. Face was complex with vertical parting, old fracture, argillaceous quartzite and a new fracture observed.

Hole No. 2: Azimuth: 317°, Inclination: -5°

It appears that the rock in hole No. 2 is softer than the rock found in hole No. 1. [Probably more argillaceous.]

Doorstopper No. 9   Depth 12'3"

Readings dropped quickly after the 14:40 readings. Two H, V, 45+ 45- have therefore been calculated. Quartzite with argillic stringers fracture occupied directly behind doorstopper. Poor bonding.

Doorstopper No. 10   Depth 19'4"

Quartzite, fractured. One vertical fracture 6 1/2" long running from D.S. to end of core. Good bond, Rock attached to D.S. is solid. Probable cause of low readings is vertical fracture.

Doorstopper No. 11   Depth 22'7"

-FAILURE- Readings were no good. 4" core, good bonding, no fractures. This doorstopper was not left for a longer period in the hole to become stable.

Doorstopper No. 12   Depth 24'7"

Good bond, fracture 2 1/2" behind doorstopper.

Doorstopper No. 13   Depth 29'0"

Good bond, no visible fractures. Pure qtzite. Overcore plot [figure C-1B] suggests last reading may be in error.

Doorstopper No. 14   Depth 31'11"

Pure Qtzite, good bond, no visible fractures, some thin argillite bands.
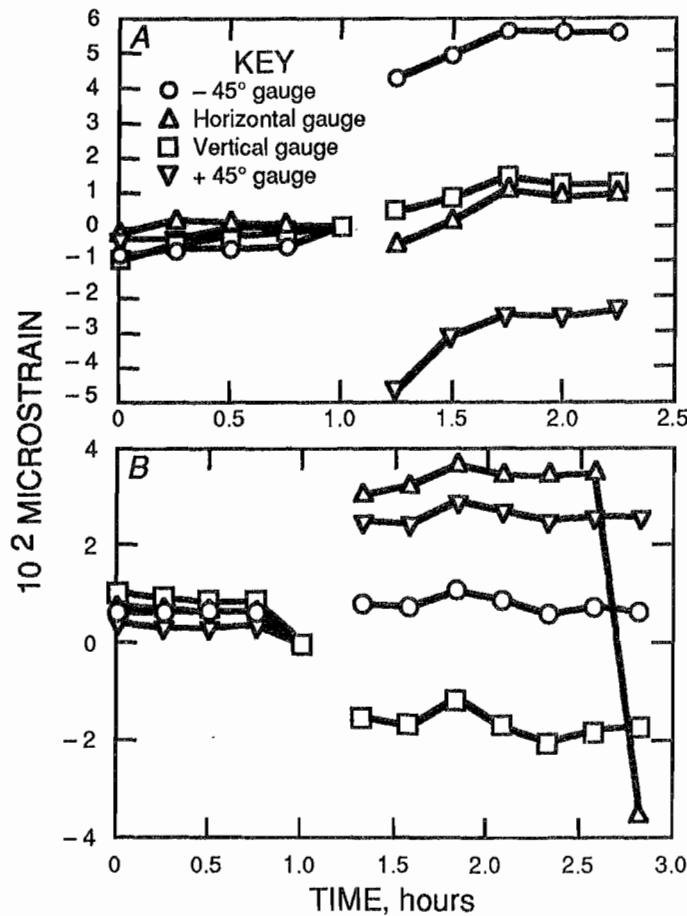
Doorstopper No. 15   Depth 35'11"

Good bond, qtzite some argillite discing occurred behind D.S. no visible fractures

Hole No. 3: Azimuth: 17°, Inclination: -5°

Doorstopper No. 16   Depth 12'6"

Appears gage is becoming sticky. Good bond, qtzite core was broken while being removed from face, no visible fractures.

Doorstopper No. 17   Depth 16'6"

Drilled thru 1 1/2' band disconnected sulfides 4' ahead of D.S. No. 2 Gage is still slightly sticking. Qrtzite, bad bonding, probably cracked attempting to remove the core after overcoring fracture 1/2" behind the D.S. developed while overcoring. Appears epoxy is not setting up, environment is changing the chemistry of the epoxy.

Doorstopper No. 18   Depth 24'4"

Bad bond, parts of core stayed in hole. Visible fractures in Rock ahead of D.S. The gage appears to still be sticking. The epoxy has changed chemically.

Figure C-1

Overcore strain plots. A, Doorstopper cell 4; B, doorstopper cell 13. The last reading for the +45° gauge on cell 13 appears to be in error.

APPENDIX D.—SENSITIVITY OF STRESS FIELD ESTIMATE
TO CHOICE OF STRESS CONCENTRATION FACTOR

Allen's (1979) six strains were used to calculate in situ stress using a variety of reported stress concentration factors. These calculations (table D-1) show the large variations in stress field estimates associated with the possible choices of stress concentration factors proposed by a number of researchers (Bonnechere and Fairhurst, 1971; Hocking, 1976; Rahn, 1984; Van Heerden, 1969). Only Allen's reported stress field reflects his misdefinition of shear strain. The resulting difference appears to be of the same order as variations resulting from recent improvements in the definition of stress concentration factors.

Table D-1.—Stress solutions based on Allen's six strains

Component	Magnitude		Bearing	Plunge	SFC	Notes
	GPa	psi				
σ_1	74	10,800	N 37° W	29°		
σ_2	47	6,800	N 56° E	3°		(^{1})
σ_3	24	3,500	S 20° E	61°		
σ_v	36	5,200				
σ_1	63	9,100	N 48° W	-3°	a = 1.25,	
σ_2	30	4,400	N 44° E	-35°	b = 0,	(^{2})
σ_3	11	1,500	N 38° E	55°	c = 0, and	
σ_v	17	2,500			d = 1.25,	
σ_1	89	13,000	N 48° E	-5°	a = 1.25,	
σ_2	64	9,200	N 45° E	-30°	b = 0,	(^{3})
σ_3	50	7,300	N 34° E	60°	c = -0.51, and	
σ_v	54	7,800			d = 1.25	
σ_1	109	15,900	N 48° W	-5°	a = 1.25,	
σ_2	85	12,400	N 45° E	-30°	b = -0.064	(^{4})
σ_3	72	10,500	N 34° E	59°	c = -0.64, and	
σ_v	76	11,000			d = 1.25	
σ_1	89	13,000	N 48° W	-5°	a = 1.34,	
σ_2	66	9,500	N 45° E	31°	b = -0.07,	(^{5})
σ_3	53	7,700	N 34° E	59°	c = -0.56, and	
σ_v	57	8,200			d = 1.41	

SFC Stress concentration factors (equations 2-4 in main text).
[1]Allen's reported stress field.
[2]STRESsOUT solution with stress concentration factors used by Allen (1979).
[3]STRESsOUT solution with stress concentration factors reported by Bonnechere and Fairhurst (1971).
[4]STRESsOUT solution with stress concentration factors developed for ν = 0.18 (after Van Heerden, 1969).
[5]STRESsOUT solution with stress concentration factors developed according to equations reported by Rahn (1984).